Non-cytotoxic polymer vesicles for rapid and efficient intracellular delivery

Hannah Lomas,†[a] Marzia Massignani,†[a] Khairuddin A. Abdullah,[a] Irene Canton,[a] Caterina Lo Presti,[a] Sheila MacNeil,[a] Jianzhong Du,[b] Adam Blanazs,[b] Jeppe Madsen,[b] Steven P. Armes,[b] Andrew L. Lewis[c] and Giuseppe Battaglia*[a]

Received 12th November 2007, Accepted 9th January 2008
First published as an Advance Article on the web 22nd April 2008
DOI: 10.1039/b717431d

We have recently achieved efficient cytosolic delivery by using pH-sensitive poly(2-(methacryloyloxy)ethylphosphorylcholine)-co-poly(2-(diisopropylamino)ethylmethacrylate) (PMPC–PDPA) diblock copolymers that self-assemble to form vesicles, known as polymersomes, in aqueous solution. It is particularly noteworthy that these diblock copolymers form stable polymersomes at physiological pH but rapidly dissociate below pH 6 to give molecularly-dissolved copolymer chains (unimers). These PMPC–PDPA polymersomes are used to encapsulate nucleic acids for efficient intracellular delivery. Confocal laser scanning microscopy and fluorescence flow cytometry are used to quantify cellular uptake and to study the kinetics of this process. Finally, we examine how PMPC–PDPA polymersomes affect the viability of primary human cells (human dermal fibroblasts (HDF)), paying particular regard to whether inflammatory responses are triggered.

Introduction

One of the most challenging aspects of drug delivery is the intracellular delivery of active agents. Anti-cancer drugs, therapeutic enzymes, and especially nucleic acids all need to be delivered within the cell interior to exert their therapeutic action. Small hydrophobic molecules can permeate cell membranes with relative ease, but hydrophilic molecules (and especially large macromolecules such as proteins and nucleic acids) require a vector to assist their transport across the cell membrane. This must be designed so as to ensure intracellular delivery without compromising cell viability. Cell entry is regulated by a complex process called endocytosis. This results in the formation of an intracellular membrane-enclosed capsule (endocytotic vesicle) *via* the infolding of the outer cellular membrane. There are several endocytosis pathways with differing internalisation mechanisms,[1,2] but each involves the internalised material experiencing a rapid drop in local pH (from neutral pH to pH 6.0 inside endocytotic vesicles, to as low as pH 5.5 inside late endosomes and lysosomes).[2]

[a]*Biomaterials and Tissue Engineering Group, Department of Engineering Materials, University of Sheffield, The Kroto Research Institute, Broad Lane, Sheffield, UK S3 7HQ. E-mail: g.battaglia@sheffield.ac.uk; Fax: +44 (0)1142225945; Tel: +44 (0)1142225962*
[b]*Department of Chemistry, University of Sheffield, Dainton Building, Brook Hill, Sheffield, UK S3 7HF*
[c]*Biocompatibles UK Ltd, Chapman House, Farnham Business Park, Weydon Lane, Farnham, Surrey, UK GU9 8QL*

† HL and MM contributed equally to this work.

Consequently, in order to achieve effective intracellular delivery, the ideal vector should be engineered to: (i) encapsulate and hence protect the therapeutic agent, (ii) survive in the extracellular space and biological fluids, (iii) bind to the cell surface, (iv) survive and escape the endocytic pathway. Apart from viral vectors, which are obviously limited to gene delivery and have various well-documented advantages and disadvantages,[3] most attempts to design an effective cytosolic delivery vector have centred around pH-sensitive liposomes,[4–6] water-soluble polymers,[7] and, recently, several types of nanoparticles,[8,9] including nanotubes.[10] Liposomes, *i.e.* vesicles formed by natural or synthetic phospholipids in water, have been investigated for several decades and some formulations have reached the market.[11] However, liposomes are often leaky, unstable and, without polymer modification,[12] have a very limited life *in vivo*.[13] In addition, although of natural origin, phospholipids can affect cellular gene expression and exhibit cytotoxicity.[14,15] Conversely, effective intracellular delivery of anti-cancer drugs has been achieved using either linear or dendrimer polymer–drug–ligand conjugates.[7] This approach has already shown that therapeutic agents have a very different effect once released *inside* cells. However, such formulations are often based on complex chemical modification and can only be used for a limited number of active agents.

Recently, polymer and liposome technologies have been combined by synthesising amphiphilic copolymers that are able to form nanometer-sized vesicles, known as polymersomes.[16,17] Such copolymers have much higher molecular weights than phospholipids and can self-assemble into tougher, more resilient[18] membranes, conferring improved mechanical properties on the final structure.[17] Moreover, the wholly synthetic nature of these copolymers allows a wide range of compositions and molecular weights to be easily targeted. By varying the copolymer molecular mass, we can adjust the mechanical properties and permeability of the polymersomes.[17,19] Because of their macromolecular nature, amphiphilic copolymers have critical aggregation concentrations (*i.e.* the minimum copolymer concentration necessary to form the aggregate) that are very low and, in some cases, essentially zero. Thus these copolymers have very slow chain exchange dynamics, implying self-assembly into locally isolated, non-ergodic structures.[20,21] Their slow rates of dissociation enable polymersomes to retain their payloads for very long time periods. Furthermore, the absence of molecularly-dissolved, amphiphilic copolymers in solution prevents cytotoxic interactions with biological phospholipid membranes. These can range from complete cellular membrane dissolution (and hence cell death), in the case of small-molecule surfactants,[22] to up-regulation of gene expression and altered cellular genetic responses.[23] These properties have recently encouraged the application of polymersomes as delivery vectors for bioactive molecules.[24–27] In principle, assuming that the copolymers have the appropriate overall hydrophile/hydrophobe balance, polymeric membranes can contain a range of different functionalities. In particular, the non-fouling and non-antigenic properties[28–30] of poly(ethylene oxide) (PEO) [also known as poly(ethylene glycol), or PEG] and poly(2-(methacryloyloxy)ethyl phosphorylcholine) (PMPC) have been combined with hydrophobic polymers in the design of biocompatible polymersomes that are expected to exhibit very long circulation times.[16,24] Stimulus-responsive polymersomes have also been designed to exploit the sensitivity of specific hydrophobic polymers to external stimuli such as pH,[31] oxidative species,[32] and hydrolysis.[33] Such polymersomes have also been decorated with ligands such as antibodies and biotin groups that allow targeting of specific biological sites.[34] Finally, we have recently demonstrated the ability of certain polymersomes to efficiently deliver DNA within cells.[27]

Herein we present the use of biomimetic polymersomes for the efficient encapsulation and intracellular delivery of active agents. These polymersomes are formed by the self-assembly of pH-sensitive AB diblock copolymers, where A = poly(2-(methacryloyloxy)ethylphosphorylcholine) [PMPC] and B = poly(2-(diisopropylamino)ethylmethacrylate) [PDPA]. The PMPC block is highly biocompatible, whilst the PDPA block imparts pH-sensitivity to the copolymer. At physiological pH, the

copolymer forms colloidally-stable, nanometer-sized polymersomes,[31] whereas below the pK_b of the PDPA block, rapid dissociation of the polymersomes occurs as the tertiary amine groups on the PDPA chains become protonated. This affords molecularly dissolved copolymer chains (unimers) as the PDPA block switches from hydrophobic at neutral pH to hydrophilic (*i.e.* a weak cationic polyelectrolyte) in mildly acidic solution.

Experimental

Materials

$PMPC_{25}$–$PDPA_{70}$ block copolymer was synthesised by atom transfer radical polymerisation (ATRP), as reported elsewhere.[31] PEO_{16}–PBO_{18} block copolymer was synthesised by sequential anionic polymerisation, as described elsewhere.[35] Rhodamine-labelled $PMPC_{30}$–$PDPA_{60}$ block copolymer was synthesised using a method reported elsewhere.[36] The pEGFP DNA construct used to prepare the GFP plasmid, and the Qiagen columns, were purchased from CLONTECH Laboratories (Palo Alto, CA) and the strain JM109 used for propagation in *Escherichia coli* and the pGL3 luciferase reporter vector were purchased from Promega UK. Luria–Bertani (LB) media, ampicillin and kanamycin solutions, *Sfi I* and ethidium bromide solution were purchased from Sigma-Aldrich (UK). Chloroform, methanol and isopropanol were purchased from Fisher Scientific, phosphate buffer saline (PBS) tablets from Oxoid Ltd, and sodium hydroxide, sepharose 4B, Rhodamine B octadecyl ester perchlorate and 4′,6-diamidino-2-phenylindole (DAPI) from Sigma-Aldrich (UK). Dulbecco's modified Eagle's medium (DMEM) and fetal calf serum were bought from Biosera (UK) and L-glutamine, penicillin streptomycin, amphotericin B and ethylenediaminetetraacetic acid (EDTA) disodium salt were bought from Sigma (UK). Collagenase A was purchased from Boehringer-Mannheim (Lewes, UK). For the MTT-ESTA assay, 3-(4,5-dimethylthiazol-2-yl)-2,5-diphenyltetrazolium bromide (MTT) was purchased from Sigma-Aldrich (UK) and hydrochloric acid from BDH AnalaR. The LiposoFast-Basic, polycarbonate membranes and gas-tight glass syringes were purchased from GC Technology (UK). For the immunolabelling of p65, the Santa Cruz anti-human p65 (c-20) rabbit polyclonal IgG and biotinylated anti-rabbit IgG antibodies, plus fluorescein–streptavidin were purchased from Vector Laboratories (Burlingame, CA). TNF-α was purchased from Roche Diagnostics Ltd (UK), and 10% formalin solution and Triton X100 were purchased from Sigma-Aldrich (UK).

GFP plasmid preparation

pEGFP DNA construct was used in DNA encapsulation studies and the strain JM109 for propagation in *E. coli*. Selection for the transformed bacteria was maintained by growing the culture at 37 °C in LB media with 100 μg kanamycin ml^{-1}. Plasmid DNA was isolated from *E. coli* JM109 using Qiagen columns. DNA purity was assessed by comparing the relative absorbances at 260 and 280 nm. The optical absorbance at 260 nm and the molar extinction coefficient were used to measure the concentration of nucleic acid present in the final solution. Restriction digests were conducted using 1 unit of *Sfi I* per μg DNA, the appropriate reaction buffer and incubation at 37 °C for 1 h according to the protocol provided by the restriction enzyme supplier. Digested plasmid, intact plasmid and λDNA molecular mass marker were run on a 1% agarose gel and stained with ethidium bromide for analysis of the purification procedure.

Luciferase plasmid preparation

pGL3 luciferase reporter vector was used to prepare the luciferase-encoding plasmid, and the strain JM109 for propagation in *E. coli*, using the protocol

described above for the GFP plasmid preparation, except the culture was grown with 100 μg ml^{-1} ampicillin, as opposed to kanamycin.

Electroformation of the polymersomes

Micrometer-sized (so-called 'giant') PMPC–PDPA polymersomes were prepared by electroformation using a TG315 (TTi) function generator. $PMPC_{25}$–$PDPA_{70}$ copolymer ($M_{n,GPC}$ = 35 200 and M_w/M_n = 1.08) was dissolved in a chloroform–methanol solution (5 : 1 v/v) reaching a concentration of 1 mg ml^{-1}. A Rhodamine-labelled fluorescent $PMPC_{30}$–$PDPA_{60}$ diblock copolymer was added to the solution at a concentration of 5.0 w/w% with respect to the total amount of PMPC–PDPA, in order to analyse the giant polymersomes by confocal laser scanning microscopy (CLSM). Two platinum electrodes of 20 mm length and 3 mm height were coated with 8 μl of the PMPC–PDPA solution and placed in a vacuum oven at 50 °C for 2 h. After drying, the two electrodes were placed in a Petri dish at a distance of 5 mm and an ac voltage of 1.4 V was applied at 10 Hz while 6 ml of PBS buffer solution (pH 7.4) was gently added. After all the PBS had been added, the voltage was increased up to 5 V at 10 Hz and kept constant until the end of the experiment. The surface of the electrodes was analysed with a LSM 510 (Zeiss) CLSM by exciting the samples at 543 nm with a HeNe laser. After formation of the giant polymersomes, 0.1 M HCl was added to the solution until the solution pH reached 5.0.

Polymersome preparation and DNA encapsulation

In a typical experiment, $PMPC_{25}$–$PDPA_{70}$ copolymer was added to a glass vial and dissolved in a solution of 2 : 1 chloroform–methanol, at a concentration of 3.0 mg ml^{-1}. This solvent mixture was evaporated under vacuum, resulting in a copolymer film being deposited on the walls of the vial. The resulting copolymer film was sterilised in an autoclave, if required, and then rehydrated using phosphate buffer saline (100 mM PBS) to form a 0.50 w/w% copolymer suspension. The pH of this suspension was lowered to pH 2, the resulting copolymer solution was stirred for 1 h, and the pH was increased to pH 6.0. For the transfection experiments, DNA plasmid was added to this aqueous polymersome solution up to a concentration that corresponded to a [DPA]–[phosphate] molar ratio of *circa* 100 : 1. The solution was then manually extruded using a LiposoFast-Basic through a polycarbonate membrane of defined pore size (200 nm), using a gas-tight glass syringe, and sonicated for 10 minutes using a sonicator (Sonicor Instrument Corporation). Polymersomes encapsulating the DNA plasmid were purified by preparative gel permeation chromatography (GPC), using a size exclusion column containing sepharose 4B and PBS eluent at pH 7.3. The DNA encapsulation efficiency was determined by the addition of 1 μg ml^{-1} 4′,6-diamidino-2-phenylindole (DAPI) to both the pure and impure polymersome solutions, followed by analysis using a Cary Eclipse Varian fluorimeter. Fluorescence emission spectra were recorded using an excitation wavelength of 350 nm for DAPI detection. In the presence of double-stranded DNA, the broad fluorescence emission peak corresponding to DAPI at approximately 460 nm increases and shifts to a slightly lower wavelength. Calibration curves were recorded at known DNA and polymersome concentrations, and subsequently used to calculate the encapsulation efficiency.

Encapsulation of octadecyl Rhodamine B

Rhodamine B octadecyl ester perchlorate was dissolved in chloroform to form a 0.5 mg ml^{-1} solution. 50 μl of this solution was added to a 20 mg sample of $PMPC_{25}$–$PDPA_{70}$ copolymer dissolved in 2 : 1 chloroform–methanol. The solvent was then evaporated under vacuum, as described above, forming thin copolymer films on the walls of the glass vials, which were subsequently sterilised in an autoclave.

The copolymer films were rehydrated in PBS, forming 0.50 w/w% copolymer suspensions. The pH of the resulting suspensions was lowered to pH 2, the solutions were stirred for 1 h, and the pH was increased to pH 7.3 for polymersome formation. The polymersome dispersions were manually extruded using a LiposoFast-Basic through a polycarbonate membrane of defined pore size (200 nm), using a gas-tight glass syringe, sonicated for 10 minutes, and then purified *via* preparative gel permeation chromatography (GPC). Those fractions that contained polymersomes loaded with amphiphilic fluorescent dye, as judged by both their turbidity and colour, were used to treat the cells.

PEO–PBO polymersome preparation and encapsulation of octadecyl Rhodamine B

PEO_{16}–PBO_{18} block copolymer was dissolved in chloroform at the concentration of 30 mg mL^{-1} in a glass vial and 0.5 mL of a 0.50 mg mL^{-1} Rhodamine solution in chloroform was added. The chloroform was evaporated in a vacuum oven, leading to the formation of a pink viscous gel at the bottom of the vial. The sample was sterilised in an autoclave before sufficient sterilised PBS was added to make up a 1.0 w/w% polymersome solution. The vial was placed on a shaker for 10 minutes. The resulting polymersome dispersion was extruded through a LiposoFast-Basic polycarbonate membrane to produce narrower polymersome particle size distributions. The solution was passed 21 times through a membrane with pore sizes of 200 nm in diameter by pushing the sample back and forth between two gas-tight glass syringes.

Transmission electron microscopy

Samples were mounted on pre-coated carbon-coated copper grids. These grids were submerged for 20 seconds into the copolymer solution and then into uranyl formate water solution (2 w/w%). Imaging was performed on a Philips CM100 instrument operating at 100 kV equipped with a Gatan 1 k CCD Camera.

Dynamic light scattering

Dynamic light scattering measurements were performed on a Brookhaven Instruments 200SM laser light scattering goniometer using a HeNe 125 mW 633 nm laser. Aqueous $PMPC_{25}$–$PDPA_{70}$ polymersomes were diluted, if necessary, with filtered PBS to a concentration of 1 mg ml^{-1} and placed into glass vials. Single scans of ten minutes exposure were performed and particle sizes were estimated using the CONTIN multiple pass method of data analysis at angles of 30°, 90° and 120°. For analysis of the colloidal stability of the polymersomes with time, correlation between the average count rate histories and correlation functions at each angle were analysed. It was investigated whether polymersome storage under different conditions affected their long-term colloidal stability. Thus two polymersome solutions of 5 mg ml^{-1} and 1 mg ml^{-1} concentration were stored at both room temperature and 4 °C. Measurements were recorded on day 1 (within 2 h of polymersome preparation), day 2 (within 24 h of polymersome preparation), day 3 (within 48 h of polymersome preparation), day 4, day 9 and finally day 90.

Cell culture

Human dermal fibroblasts (HDF) were isolated from skin obtained from abdominoplasty or breast reduction operations (according to ethically-approved local guidelines, NHS Trust, Sheffield, UK). Primary cultures of fibroblasts were established as previously described.[37] Briefly, the epidermal layer of the skin was removed by trypsinisation and the remaining dermal layer was washed in PBS. The dermis was then minced using surgical blades and incubated in 0.5% (w/v) collagenase A at 37 °C overnight in a humidified CO_2 incubator. A cellular pellet was collected from the digest and cultured in DMEM (Sigma, UK) supplemented with 10%

(v/v) foetal calf serum, 2 mM L-glutamine, 100 IU ml^{-1} penicillin, 100 mg ml^{-1} streptomycin and 0.625 μg ml^{-1} amphotericin B. Cells were sub-cultured routinely using 0.02% (w/v) EDTA and used for experimentation between passages 4 and 9.

Assessment of the effect of the polymersomes on the cellular metabolic activity *via* MTT-ESTA assay

HDF cells were seeded in standard 24 well plates at a density of 3×10^4 cells per well and grown for two days in culture medium (see above). Cell monolayers were treated for 24 h with four different concentrations of $PMPC_{25}$–$PDPA_{70}$ polymersomes (0.1 mg ml^{-1}, 1 mg ml^{-1}, 2 mg ml^{-1} and 5 mg ml^{-1} in fresh culture medium). Viable cell density was then assessed using the MTT (3-(4,5-dimethylthiazol-2-yl)-2,5-diphenyltetrazolium bromide)-ESTA assay. Briefly, both treated and untreated cells were washed thoroughly twice with PBS and incubated in MTT solution (0.5 mg ml^{-1} MTT in PBS, 1 ml per well of a 24 well plate or per cm^2 of cultured cells) for 40 minutes at 37 °C and a humidified atmosphere of 5% CO_2. Dehydrogenase activity in the cells reduces MTT, forming a purple formazan salt, which is eluted from the cells using acidified isopropanol (0.4 ml per well of a 24 well plate). After 5 minutes incubation at room temperature, the acidified isopropanol from each well was transferred to a 96 well plate, and the optical density at 540 nm was measured using a plate reading spectrophotometer (Dynex Technologies, MRX II).

Live–Dead viability/cytotoxicity assay

1.5 μl of Syto 9 green and 1.5 μl propidium iodide red were mixed with 0.5 ml of normal culture medium. They were then added to the cell monolayers and incubated for 15 minutes. Before visualisation using an epifluorescence microscope (ImageXpress; Axon Instruments/Molecular Devices, Union City, CA, USA) wells were rinsed three times with PBS.

Immunolabelling of NFκ-B (p65)

HDF cells were seeded in standard 24 well plates at a density of 3×10^4 cells per well and grown for 2 days in culture medium (see above), or until 60% confluent. As a positive control, the cells were stimulated with TNF-α (1000 U ml^{-1}) in fresh culture media for 1 h. As a negative control, cells were treated with PBS, diluted 1 in 10 in fresh culture media. The cells were also stimulated for 2.5 h at 37 °C and a humidified atmosphere of 5% CO_2 with a $PMPC_{25}$–$PDPA_{70}$ polymersome solution prepared in PBS, diluted 1 in 10 in culture media. The final polymersome concentration in culture media used to treat the cells was 2 mg ml^{-1}. Each of the experiments was performed in triplicate. The reactions were stopped by removing the media and washing the cells with PBS. The cells were then fixed *in situ* with 4% (v/v) paraformaldehyde (1 ml per well of a 24 well plate) for 30 minutes and washed three times with PBS. The cell membranes were permeabilised by the addition of 0.1% (v/v) Triton X100 (in PBS) (200 μl per well), to allow antibodies to access the transcription factor NFκ-B. Again, the cells were washed three times with PBS before any unreacted binding sites were blocked with 5% (w/v) dried milk powder (in PBS) (1 ml per well) for 1 h. The cells were washed three times with PBS and the primary antibody anti-human p65 (c-20) rabbit polyclonal IgG (1 : 100 (v/v) in blocking buffer) was added (300 μl per well). The blocking buffer used this time was a 1% (w/v) dried milk powder solution in PBS. The cells were incubated on a rocker for 1 h at room temperature. On removal of the primary antibody, the cells were washed three times with PBS and 300 μl per well of the secondary antibody was added to the cells (1 : 1000 (v/v) in blocking buffer). The secondary antibody used was a biotinylated antibody that is anti- to the animal which raised the primary antibody. The same conditions were applied for the secondary antibody as for the primary. The cells were washed three times with PBS and treated with the tertiary label

fluorescein–streptavidin (1 : 100 (v/v) in PBS) for 30 minutes at room temperature. The cells were subsequently imaged in PBS using an epifluorescence microscope (ImageXpress; Axon Instruments/Molecular Devices, Union City, CA, USA). For fluorescein detection, λ_{ex} 495 nm and λ_{em} 515 nm were used at an exposure of 1000 ms.

Intracellular delivery of octadecyl Rhodamine B, analysis by CLSM and fluorescence flow cytometry measurements

The HDF cell monolayers were incubated with PEO–PBO and PMPC–PDPA polymersomes encapsulating octadecyl Rhodamine B and, after different time periods, washed three times with PBS before being imaged in PBS using CLSM. For fluorescence flow cytometry measurements, the cells were trypsinised using EDTA, a cellular pellet was collected, and the cells were resuspended in PBS.

Transfection of HDF cells

Standard 24 well plates were seeded at a density of 3×10^4 cells per well for the HDF cells, and grown for two days in culture media (see above). Cells were replenished with fresh media (1 ml) 3 h prior to transfection. Transfection media were then prepared in normal culture media by mixing with $PMPC_{25}$–$PDPA_{70}$ polymersomes containing the luciferase-encoding plasmid. Polymersomes were investigated in transfection assays at 0.5 mg ml^{-1} (this corresponds to 0.7 μg ml^{-1} of plasmid DNA). Cells were incubated in transfection media for 24 h in a humidified CO_2 incubator. Thereafter, the cell monolayers were washed three times with PBS and fresh culture media was added.

Luciferase assay

Luciferase assay reagent and lysis buffer (Promega) were prepared prior to analysis. Lysis buffer was added to the cell monolayers, and they were placed at −80 °C for 1 h. After this time period, wells were allowed to defrost and the buffer was added to luciferase assay reagent to calculate the amount of protein production using a luminometer.

Results and discussion

pH-Induced dissociation of polymersomes into unimers

Polymersomes were formed using $PMPC_{25}$–$PDPA_{70}$ diblock copolymers comprising a non-fouling PMPC block and a pH-sensitive ($pK_b \sim 5.8$–6.6, depending on the ionic strength[38]) poly(2-(diisopropylamino)ethylmethacrylate) (PDPA) block, where the subscripts denote the respective mean degrees of polymerisation. Below the pK_b of the PDPA chains, most of the tertiary amine groups are protonated and therefore cationic, while above this pK_b these amines are largely deprotonated and highly hydrophobic. PMPC–PDPA copolymers were recently reported[31] to form stable polymersomes at physiological pH; rapid dissociation of these polymersomes occurs in acidic solution to form molecularly dissolved copolymer chains (unimers). Both morphologies are shown by TEM and DLS in Fig. 1a–d. It is important to notice that both TEM and DLS show the two extreme morphologies; copolymers are either molecularly dissolved at pH 6 or self-assemble into polymersomes at pH 7. In order to understand the details of this phase transition, we prepared micrometer-sized polymersomes by electroformation according to a previously published protocol.[18,39] Fluorescent Rhodamine-labelled $PMPC_{30}$–$PDPA_{60}$ diblock copolymers were mixed with non-labelled $PMPC_{25}$–$PDPA_{70}$ up to 5.0 w/w%, in order to analyse the polymersomes by confocal laser scanning microscopy (CLSM). After polymersome formation, 0.1 M HCl was added dropwise to the aqueous solution until the solution

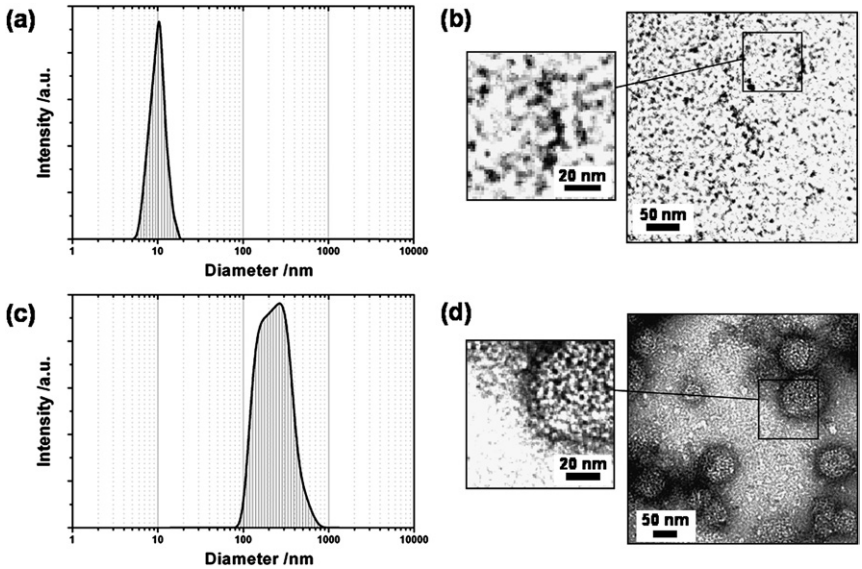

Fig. 1 (a) DLS particle size distribution of PMPC–PDPA unimers at pH 6. (b) TEM micrograph of PMPC–PDPA unimers at pH 6. (c) DLS particle size distribution of PMPC–PDPA polymersomes formed at pH 7. (d) TEM micrograph of the PMPC–PDPA polymersomes.

pH reached 5.0. A representative PMPC–PDPA polymersome is reported in Fig. 2. Immediately after HCl addition, stable pores are visible in the polymersome membrane. These pores enlarge while the polymersomes dissolve and shrink, until complete membrane disruption occurs. This phase change is complete within five minutes. Although the phase transition from polymersomes to unimers takes only a few minutes, the observation of pore formation suggests essentially instantaneous release of the polymersome payload. Similar transitions were observed by Bocher *et al.* for related pH-sensitive polymersomes.[40] It also important to note that, once formed, these polymersomes are stable for at least three months at room temperature. Fig. 3 confirms that the correlation functions measured by DLS at different ageing times are almost identical, indicating that the polymersome particle size distribution does not change with time.

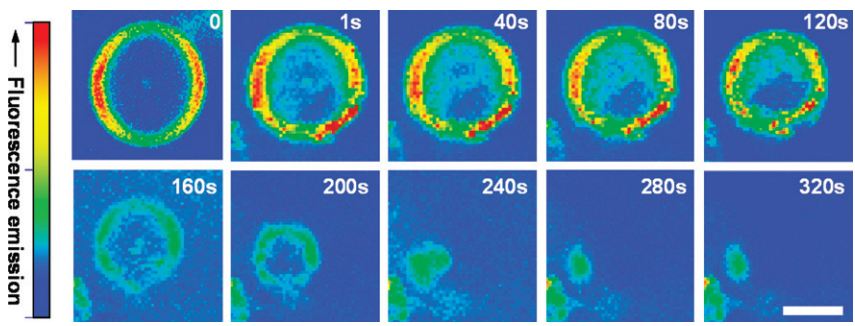

Fig. 2 Confocal laser scanning micrographs of micrometer-sized PMPC–PDPA polymersomes formed by electroformation. Immediately after the addition of 0.1 M HCl, pores are visible within the polymersome membrane. Subsequent solubilization and shrinking of the polymersomes was observed until complete disruption occurred. Note: at time zero the anisotropy of the apparent fluorescence intensity around the circumference is an optical artefact due the large vesicles no longer being buoyant. The graph bar corresponds to 20 micrometers.

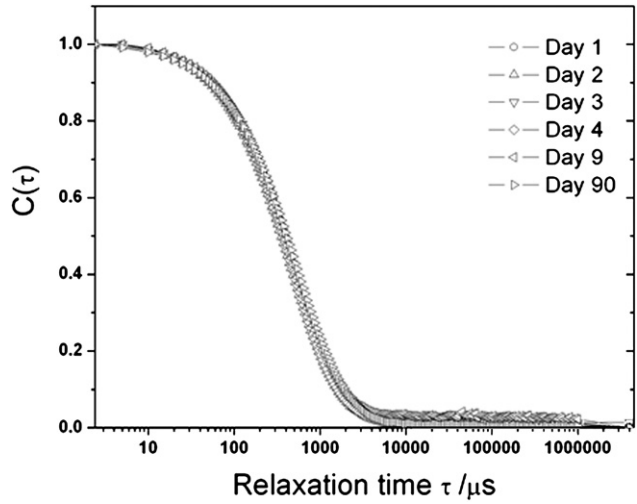

Fig. 3 DLS correlation functions determined for aged PMPC–PDPA polymersomes after different time periods (mean polymersome diameter was approximately 200 nm in each case).

Interactions of the polymersomes with cells

The effect of $PMPC_{25}$–$PDPA_{70}$ polymersomes on cellular metabolic activity was assessed using an MTT-eluted stain assay (ESTA). This is based on the reduction of the MTT (3-(4,5-dimethylthiazol-2-yl)-2,5-diphenyltetrazolium bromide) by the cellular dehydrogenase enzymes. The enzyme activity can be approximately related to the number of viable cells.[41] Human dermal fibroblast (HDF) cell monolayers were treated for 24 h with four different concentrations of the $PMPC_{25}$–$PDPA_{70}$ copolymer. The data shown in Fig. 4a show the cell viabilities compared to the control sample, which is arbitrarily taken to be 100%. PMPC–PDPA polymersomes had almost no effect on the HDF cell viability. The viability study was also extended in time and the HDF cells were exposed to PMPC–PDPA polymersomes for up to one week. The fluorescent micrographs in Fig. 4b show HDF cells stained using a Live–Dead viability/cytotoxicity assay (Invitrogen, kit L-7013). This comprises a membrane-permeant dye that labels the nucleic acids of live cells with green fluorescence, and a membrane-impermeant red dye that labels nucleic acids of

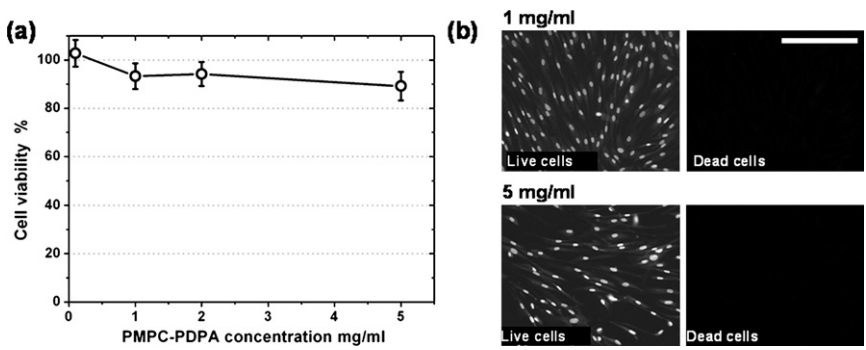

Fig. 4 (a) MTT-ESTA cell viability assay of HDF cells incubated with different concentrations of PMPC–PDPA polymersomes. (b) Live–Dead staining of HDF cells after incubation with 1 mg ml^{-1} and 5 mg ml^{-1} PMPC–PDPA polymersomes for one week. The graph bar corresponds to 100 micrometers.

membrane-compromised cells with red fluorescence. As is evident from the Figure, no dead cells were observed even after a week's exposure at a copolymer concentration of 5 mg ml^{-1}. It is worth emphasizing that membrane-forming copolymers only assemble into polymersomes at concentrations lower than 10 mg ml^{-1}; at higher concentrations more complex lyotropic phases are formed.[42] The cytotoxicity data thus confirm that, within the concentration range over which polymersomes exist, their effect on the cell viability is negligible.

In addition to these cell viability studies, we examined whether $PMPC_{25}$–$PDPA_{70}$ polymersomes, although non-toxic, triggered any cellular inflammatory response. The presence of inflammation would be indicative of negative interactions between the exogenous particle (*e.g.* the polymersomes) and the cells. The inflammatory response was tested on HDF cells by immunolabelling one of the subunits (p65) that comprises the transcription factor NF-κB. This transcription factor can be activated by exposure of cells to bacterial endotoxins (*e.g.* lipopolysaccharide (LPS)), inflammatory cytokines (*e.g.* TNF or IL-1), viral infection or expression of certain viral gene products, UV irradiation, B or T cell activation, and by other physiological and non-physiological stimuli.[43] In its inactive form, NF-κB is located in the cell cytoplasm, but is translocated into the nucleus upon its activation where NF-κB dimers bind to target DNA elements and activate transcription of genes encoding proteins involved with immune or inflammatory responses and with cell growth control.[43] Immunolabelling of p65 is undertaken by the addition of a biotinylated antibody, which binds to the transcription factor, followed by the addition of streptavidin–FITC, which strongly binds to the biotinylated antibody. The FITC label allows detection of the intracellular location of the transcription factor using a fluorescence microscope (Fig. 5a). As a positive control, cells were stimulated using the pro-inflammatory agent TNF-α (10 ng ml^{-1}). The translocation of NF-κB to the nuclei of cells treated with cytokine TNF-α is an indication of the cells responding to stress. In this event all the cell nuclei fluoresce as a consequence of the nuclear localisation of the NF-κB as shown in Fig. 5a. A solution of phosphate buffered saline (PBS) was used as the negative control. In this case NF-κB is in its inactive form and therefore only located within the cell cytosol, hence the cell nuclei do not fluoresce. When cells have been exposed to PMPC–PDPA polymersomes (2 mg ml^{-1}), no fluorescence is seen in the cell nuclei. This indicates that the NF-κB is still in its inactive form. Quantification is possible by counting cells (sampling 10 micrographs per sample) and determining the percentage that have been stimulated. The bar chart in Fig. 5b shows that at the copolymer concentration investigated, and relative to the negative control, the polymersomes do not trigger an inflammatory response from the HDF cells.

More insights into the interactions between PMPC–PDPA polymersomes and cells can be gained by studying the internalisation of the polymersomes by

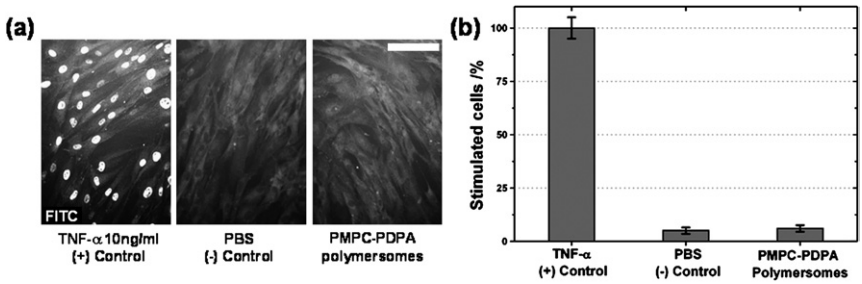

Fig. 5 (a) and (b) Investigation of the possible pro-inflammatory effect of PMPC–PDPA polymersomes on HDF cells, as assessed by immunolabelling of NF-κB. Relative to the PBS negative control and the cytokine TNF-α positive control, these polymersomes do not stimulate an inflammatory response in this cell type. The graph bar corresponds to 50 micrometers.

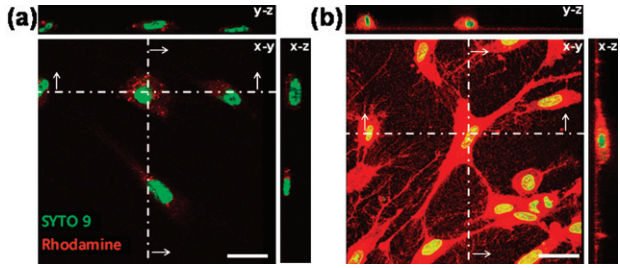

Fig. 6 *Z*-Stack confocal laser scanning micrographs of HDF cells showing intracellular delivery of octadecyl Rhodamine B by (a) non-pH-sensitive PEO–PBO polymersomes and (b) pH-sensitive PMPC–PDPA polymersomes. The cell nuclei have been stained using Syto 9. The graph bars corresponds to 50 micrometers.

HDF cells. This was assessed by encapsulation of octadecyl Rhodamine B inside the polymersomes. This amphiphilic fluorescent dye is a very efficient stain for the polymersome membrane[18,44] and therefore allows polymersome tracking by fluorescence microscopy. HDF cells were incubated with both Rhodamine-loaded non pH-sensitive poly(ethyleneoxide)–poly(butyleneoxide) (PEO–PBO) polymersomes (Fig. 6a) and pH-sensitive PMPC–PDPA polymersomes (Fig. 6b), and washed with PBS prior to imaging using CLSM operating at variable depths of focus. The images are then stacked together to form orthonormal projections that allow visualisation of cells in the *x*–*y*, *x*–*z*, and *y*–*z* planes. No significant fluorescence was detected for control samples incubated either with octadecyl Rhodamine B alone or with non-stained polymersomes. Although both types of polymersome are clearly internalised by the cells, the fate of the loaded Rhodamine is very different in the two cases. When delivered by non-pH-sensitive polymersomes, the Rhodamine is concentrated around the nuclei, most likely the cell lysosomes, while the Rhodamine stains almost all the cell cytosol when delivered by the pH-sensitive PMPC–PDPA polymersomes. Assuming that polymersomes are internalised by endocytosis, it is essential that, in order for active agents to reach their target organelle, the polymersomes can escape the endocytic pathway. The pH-sensitivity of the PMPC–PDPA polymersomes is essential to ensure endosome escape. The pH of the extracellular environment is approximately pH 7.3, therefore the PMPC–PDPA copolymers self-assemble into polymersomes. Regardless of the endocytic pathway that the polymersomes follow, upon internalisation, they are engulfed into a lipid organelle, the lumen of which experience a rapid pH drop *via* an influx of hydrogen ions by ATP-driven H^+ pumps.[1] This jump from neutral pH to acidic pH triggers dissociation of the PMPC–PDPA polymersomes due to protonation of the PDPA block. The increase in the number of particles created as the polymersomes dissociate into individual copolymer chains creates a large increase in the osmotic pressure of the endosome, eventually leading to its lysis and hence release of its contents into the cell cytosol.

Polymersomes, like all vesicular structures, can encapsulate a relatively large quantity of water-soluble species and, as the vesicular membrane is broken, these solutes are rapidly released. For example, in a typical experiment PMPC–PDPA polymersomes were formed in 100 mM PBS solution, hence a 200-nm polymersome comprising 1.7×10^3 copolymer chains[45] will contain around 5×10^5 ionic species. Thus dissociation converts a single polymersome into more than half a million molecular species. As any cell-internalised materials will be contained within a semi-permeable phospholipid membrane (*i.e.* an endocytic vesicle, phagosome, endosome or a pinosome), such an increase in particle number will correspond to a substantial osmotic pressure shock, since this colligative property depends uniquely on the number of particles, rather than their nature. According to the ideal solution law, the osmotic pressure, Π, can be calculated as

$$\Pi = \frac{N_{\text{particles}}}{N_A V_m} RT \quad (1)$$

where $N_{\text{particles}}$ is the number of particles, N_A is Avogadro's number, V_m is the endocytic vesicle/endosome/pinosome or phagosome volume, R is the ideal gas constant, and T is the temperature in Kelvin. Therefore, if contained in a 1 μm^3 phospholipid membrane, the pH-induced phase transition from one polymersome to half a million particles produces a 2.5 kPa osmotic pressure shock. This should be more than sufficient to generate the phospholipid membrane lysis. Previous studies[46,47] on unilamellar phospholipid vesicles have shown that lipid membrane lysis requires an osmotic shock of 0.5–2 Pa per μm^3 of vesicle volume depending on the type of phospholipid. PEO–PBO polymersomes are, in contrast, not affected by changes in pH, and therefore cannot escape the endocytic pathway and successfully deliver active agents intracellularly. On cellular uptake of the non-pH-sensitive polymersomes *via* the endocytic pathway, polymersome dissociation does not occur. There is therefore no increase in particle number and subsequent build-up of osmotic pressure inside the endosome when using PEO–PBO polymersomes as intracellular delivery vehicles, and these polymersomes are consequently unable to escape the endocytic pathway. Thus, after their uptake by HDF cells, Rhodamine-loaded PEO–PBO polymersomes can be mainly observed within the perinuclear region by CLSM, still contained within endocytic vesicles, and possibly the cell lysosomes.

Further insights into the differences between the cellular uptake of PMPC–PDPA polymersomes and PEO–PBO polymersomes were obtained by investigating the levels of cellular uptake of Rhodamine-stained polymersomes by HDF cells after different incubation times. The cells were incubated with Rhodamine-loaded polymersomes at 37 °C in a humidified CO_2 incubator. After different time periods, the cell monolayers were washed three times with PBS before being visualised by epifluorescence microscopy. Fig. 7a displays epifluorescence micrographs of HDF cells showing intracellular delivery of Rhodamine-loaded $PMPC_{25}$–$PDPA_{70}$ polymersomes. Just 1 min after the addition of the polymersomes to the cell monolayers, intracellular Rhodamine is clearly visible under the fluorescence microscope (using an excitation λ of 580 nm and an emission λ of 650 nm for Rhodamine detection) in the cell cytosol.

Comparison between the kinetics of cellular uptake by HDF cells of PMPC–PDPA polymersomes and PEO–PBO polymersomes was conducted using Rhodamine-stained polymersomes in both cases, and taking fluorescence flow cytometry measurements as a function of incubation time. The cellular uptake was measured in terms of both the % of cells that had taken up the polymersomes (Fig. 7b) and the fluorescence intensity per cell (Fig. 7c), which correlated to the amount of polymersomes that each cell had internalised. Fig. 7b clearly shows that, compared to the PEO–PBO polymersomes, the PMPC–PDPA polymersomes are rapidly internalised. After the HDF cells had been incubated for just 1 h with the Rhodamine-loaded PMPC–PDPA polymersomes, cellular uptake had reached a plateau value, and approximately 95% of the cells had taken up the polymersomes. In contrast, no intracellular uptake of the PEO–PBO polymersomes was detected for incubation times of up to 5 h with the HDF cells. This difference is due to the favourable interactions of the biomimetic PMPC block, located in the corona of PMPC–PDPA polymersomes, with the cellular plasma membrane. The PMPC–PDPA polymersomes are highly compatible with the cell surface, allowing their rapid internalisation *via* an endocytic pathway. Polymersomes that contain PEG (or PEO) in their hydrophilic corona cannot interact as readily with the cell surface membrane and consequently display a much slower rate of cellular internalisation by HDF cells (Fig. 7b). Moreover, Fig. 7c shows that, even at 92% cellular uptake after 72 h, the fluorescence intensity per cell is very low compared to that for

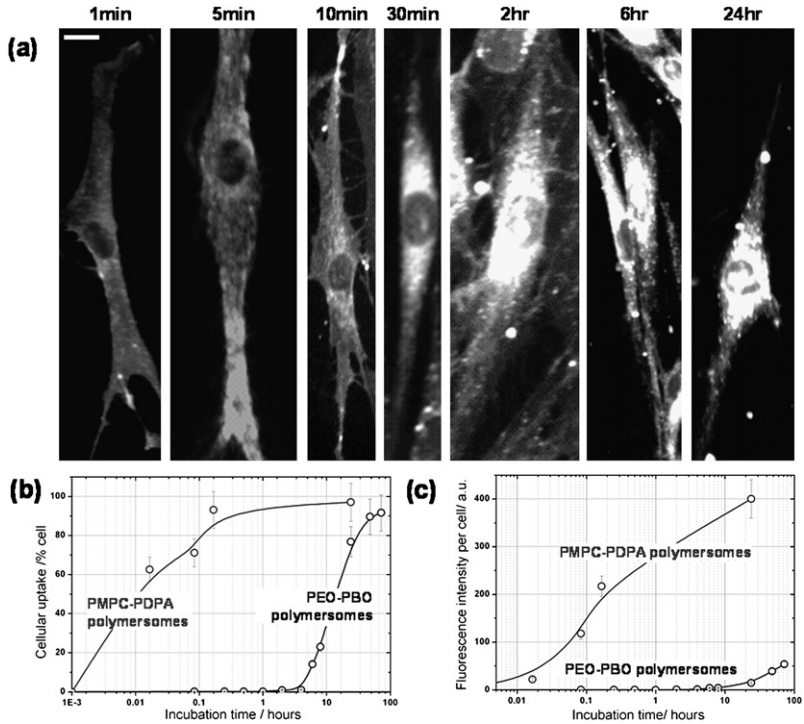

Fig. 7 (a) Fluorescence micrographs showing the uptake of Rhodamine-loaded PMPC–PDPA polymersomes at different incubation times by HDF cells; (b) and (c) fluorescence flow cytometry data showing the cellular uptake and the intensity per cell for both PMPC–PDPA and PEO–PBO polymersomes as a function of incubation time. The graph bars corresponds to 20 micrometers.

the PMPC–PDPA polymersomes. This again indicates that the PEO–PBO polymersomes do not interact as favourably with the cell surface membrane, and are therefore not internalised as readily.

DNA encapsulation and delivery

$PMPC_{25}$–$PDPA_{70}$ polymersomes have been used to successfully encapsulate plasmid DNA and subsequently deliver DNA intracellularly.[27] The interactions between plasmid DNA and PMPC–PDPA diblock copolymers have been characterised as a function of pH *via* ethidium bromide displacement assays, zeta potential measurements, dynamic light scattering (DLS) and transmission electron microscopy (TEM).[27] These techniques confirm that copolymer self-assembly into polymersomes at neutral pH is not affected by the presence of DNA and that the nucleic acid can be physically encapsulated within the aqueous cores of the polymersomes. At weakly acidic pH (*i.e.* at pH values below the pK_b of the PDPA chains), the copolymer interacts strongly with DNA, *via* electrostatic complexation between the cationic tertiary amine groups on the protonated PDPA chains and the anionic phosphate groups on the plasmid DNA, leading to the formation of a copolymer–DNA complex. Addition of plasmid DNA to the copolymer at weakly acidic pH led to an encapsulation efficiency of approximately 20%.[27] Successful transfection of HDF cells and an animal cell line (Chinese hamster ovary [CHO] cells) has recently been achieved using GFP-encoding plasmid DNA loaded into PMPC–PDPA polymersomes.[27] The resulting transfection data are very encouraging compared to the use of more traditional systems such as Lipofectamine™ and calcium phosphate

particles. Both the lipid formulation and the inorganic salt, as well as most of the non-viral gene delivery systems currently available, often cause cytotoxicity, which inevitably compromises transfection efficiency. On the contrary, the PMPC–PDPA polymersomes have very little effect on the cell metabolic activity, yet lead to high transfection efficiencies.

In order to ensure that we can consistently achieve a high transfection efficiency using PMPC–PDPA polymersomes to deliver DNA, we have optimised the encapsulation of the GFP-encoding plasmid into the polymersomes. In addition, a new technique has been developed to assess the encapsulation efficiency: after DNA encapsulation, the polymersomes are purified by preparative gel permeation chromatography (GPC). 4′,6-Diamidino-2-phenylindole (DAPI) is then added to both the purified and impure aqueous polymersome solutions, and fluorescence emission spectra are recorded using an excitation λ of 350 nm for DAPI detection. In the presence of double-stranded DNA, the broad fluorescence emission peak corresponding to DAPI at approximately 460 nm increases and shifts to a slightly lower wavelength (see Fig. 8a). Thus this DAPI assay can be used as an effective tool to assess the extent of DNA encapsulation within the polymersomes and also to determine the concentration of entrapped DNA. Fig. 8b was recorded at a DAPI concentration of 1 μg ml^{-1}. Under these assay conditions, there is a linear relationship between the DNA concentration and the fluorescence emission intensity, hence a large separation in the fluorescence emission intensity can be achieved at different DNA concentrations.

We investigated the effects of various methods of polymersome preparation on the plasmid DNA encapsulation efficiency. To obtain a reasonably narrow particle size distribution, the polymersomes were then extruded through a polycarbonate membrane with pore diameters of either 200 or 400 nm. After extrusion, the effect of polymersome sonication on DNA encapsulation efficiency was also investigated (see Fig. 9). Polymersome sonication significantly improves the encapsulation efficiency, which was as high as 25.4% for extruded polymersomes under optimal conditions. Sonication for relatively long time periods typically results in a more homogeneous polymersome distribution compared to non-sonicated polymersomes. However, sonication for too long a time period may cause degradation of the plasmid DNA. Extrusion also results in a higher encapsulation efficiency. These optimised conditions will be used to produce plasmid DNA-loaded PMPC–PDPA polymersomes for future transfection experiments.

The luciferase encoding plasmid (pGL3) has also been successfully encapsulated within PMPC–PDPA polymersomes and delivered into HDF cells. In the presence of luciferin, luciferase catalyses an oxidation reaction that is accompanied by light

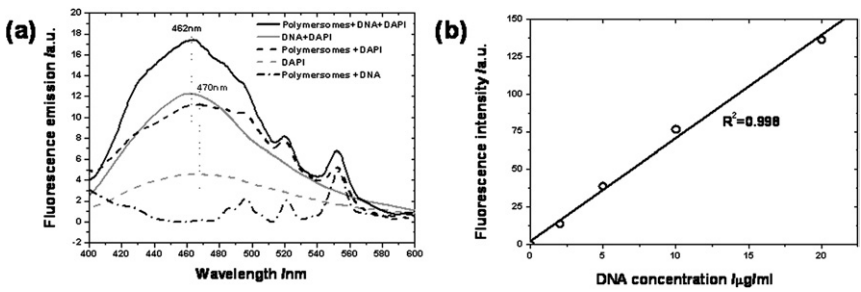

Fig. 8 DNA encapsulation within PMPC–PDPA polymersomes. (a) Fluorescence emission spectra used to determine the extent of DNA encapsulation after preparative GPC purification of the DNA-loaded polymersomes. Compared to the fluorescence emission spectrum of DAPI alone, the DAPI peak intensity increases in the presence of DNA and also shifts to a slightly lower emission wavelength. (b) Calibration graph showing that the addition of 1 μg ml^{-1} DAPI to polymersome–DNA aqueous solutions resulted in a linear relationship between the fluorescence emission intensity and the DNA concentration.

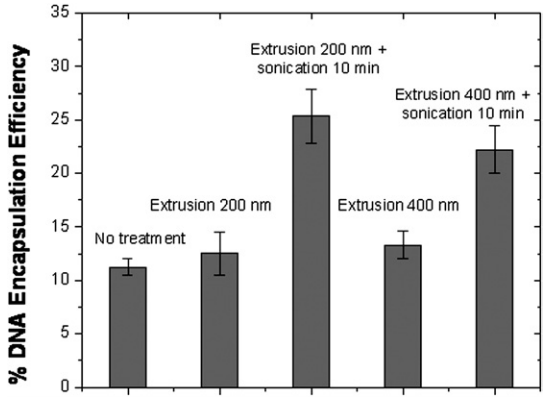

Fig. 9 Analysis of the DNA encapsulation efficiency using various PMPC–PDPA polymersome preparation methods. The encapsulation efficiency was measured by the addition of 1 μg ml^{-1} DAPI to both impure and purified aqueous polymersome solutions. These data indicate that the optimal conditions for DNA encapsulation are the formation of polymersomes of 200 nm in diameter with a relatively narrow size distribution *via* extrusion, followed by sonication for 10 min.

emission. This emitted light can be detected by a luminometer, and the transfection efficiency can therefore be assessed by quantification of the luminescence. As for GFP, the luciferase protein is only expressed if the pGL3 plasmid has been successfully incorporated into the cell nucleus, and its expression is therefore a direct indicator of the transfection efficiency. Fig. 10a shows that when $PMPC_{25}$–$PDPA_{70}$ polymersomes are used to deliver pGL3 into HDF cells, relatively high transfection efficiencies were obtained compared to negative controls (*i.e.* empty PMPC–PDPA polymersomes and the luciferase-encoding plasmid alone). Furthermore, according to the data shown in Fig. 4, we know that PMPC–PDPA polymersomes are non-cytotoxic with respect to HDF cells over the entire concentration range within which unilamellar polymersomes exist. It is important to minimise cellular toxicity due to either the transfection agent itself or the transfection agent–DNA complexes to ensure optimal transfection efficiency for *in vitro* experiments. This is also essential for avoiding adverse side effects for future *in vivo* translation. Fig. 10b shows that, once encapsulated inside the PMPC–PDPA polymersomes, plasmid DNA can remain entrapped for at least two weeks. This is confirmed by the observation that there is no loss in luminescence intensity, *i.e.* luciferase expression, for transfection experiments continued for up to 15 days after the luciferase-encoding plasmid was initially encapsulated inside the polymersomes. This indicates that, if stored

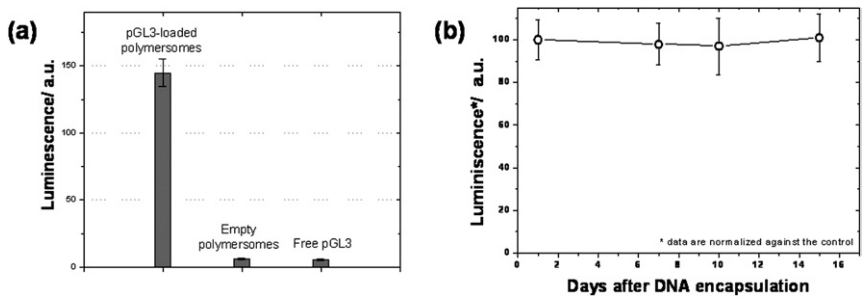

Fig. 10 (a) pGL3 transfection efficiency in human primary cells (HDF) after DNA delivery by PMPC–PDPA polymersomes. (b) pGL3 transfection efficiency in HDF cells after DNA delivery by PMPC–PDPA polymersomes, up to 15 days after their preparation and loading.

at 4 °C, the polymersomes retain their colloidal stability and there is no significant loss of encapsulant due to 'leaky' vesicular membranes. This means that transfection experiments can be routinely conducted at least two weeks after preparation of the plasmid DNA-loaded polymersomes.

Conclusions

In summary, we describe a novel non-cytotoxic synthetic vector for the rapid and efficient intracellular delivery of active agents. This vector comprises a well-defined, low polydispersity PMPC–PDPA diblock copolymer that self-assembles into polymersomes in aqueous solution at neutral pH. Such polymersomes possess very good colloidal stability on storage at ambient temperature for at least three months. Plasmid DNA can be efficiently encapsulated within the aqueous polymersome cores, with an encapsulation efficiency of at least 25% under the optimal encapsulation conditions. Furthermore, these PMPC–PDPA polymersomes can retain encapsulated DNA for at least two weeks, indicating that their membranes have a very low degree of 'leakiness'. At endocytic pH, the polymersomes dissociate due to the protonation of tertiary amine groups on the PDPA chains. This leads to the formation of DNA–copolymer complexes. These two different copolymer nanostructures (*i.e.* polymersomes at neutral pH and DNA-copolymer complexes at endocytic pH) ensure protection of plasmid DNA. The DNA–copolymer complex protects the plasmid after internalisation of the polymersomes by endocytosis. At neutral pH, the DNA is entrapped within the aqueous polymersome cores and therefore protected from blood plasma proteins. The DNA-loaded polymersomes also have stealth-like properties due to the presence of the highly biocompatible PMPC chains in the vesicular corona. This biomimetic surface minimises any interactions with blood plasma proteins, and hence extends the mean polymersome circulation time in the blood. We have already demonstrated that the polymersomes can deliver plasmid DNA intracellularly, with relatively high transfection efficiencies compared to more common *in vitro* transfection agents such as Lipofectamine™ and calcium phosphate particles.[27] This is largely due to the low cytotoxicity and absence of any pro-inflammatory response displayed by these polymersomes compared to other non-viral vectors. These highly desirable properties, together with the low degree of membrane leakiness, the biomimetic surface character of the polymersomes, and their rapid cellular uptake based on our preliminary studies with HDF cells, suggests that these new PMPC–PDPA polymersomes are excellent candidates for the intracellular delivery of a DNA.

Acknowledgements

The authors thank Professor Anthony J. Ryan and Dr Christine M. Fernyhough (Dept. of Chemistry, University of Sheffield) for supplying the PEO–PBO block copolymers, and Daniel Blakeway (Dept. of Engineering Materials, University of Sheffield) for his contribution to the work on the encapsulation of DNA into PMPC–PDPA polymersomes. We also acknowledge the Department of Engineering Materials, University of Sheffield for funding part of this work. SPA is the recipient of a Royal Society-Wolfson Research Merit Award.

References

1 S. D. Conner and S. L. Schmid, *Nature*, 2003, **422**, 37.
2 B. Alberts, A. Johnson, J. Lewis, M. Raff, K. Roberts, and P. Walter, *Molecular Biology of the Cell*, Garland Science, 2002.
3 C. E. Thomas, A. Ehrhardt and M. A. Kay, *Nat. Rev. Genet.*, 2003, **4**, 346.
4 M. B. Yatvin, W. Kreutz, B. A. Horwitz and M. Shinitzky, *Science*, 1980, **210**, 1253.
5 R. M. Straubinger, N. Düzgünes and D. Papahadjopoulos, *FEBS Lett.*, 1985, **179**, 148.
6 C.-J. Chu, J. Dijkstra, M.-Z. Lai, K. Hong and F. C. Szoka, *Pharm. Res.*, 1990, **7**, 824.

7 R. Duncan, *Nat. Rev. Drug Discovery*, 2003, **2**, 347.
8 J. Panyama and V. Labhasetwar, *Adv. Drug Delivery Rev.*, 2003, **55**, 329.
9 J. K. Vasira and V. Labhasetwar, *Adv. Drug Delivery Rev.*, 2007, **59**, 718.
10 K. Kostarelos, L. Lacerda, G. Pastorin, W. Wu, S. Wieckowski, J. Luangsivilay, S. Godefroy, D. Pantarotto, J.-P. Briand, S. Muller, M. Prato and A. Bianco, *Nat. Nanotechnol.*, 2006, **2**, 108.
11 D. D. Lasic and D. Papahadjopoulos, *Medical Applications of Liposomes*, Elsevier, 1998.
12 D. D. Lasic, *Angew. Chem., Int. Ed. Engl.*, 1994, **33**, 1685.
13 M. Hashida, R. I. Mahato, K. Kawabata, T. Miyao, M. Nishikawa and Y. Takakura, *J. Controlled Release*, 1996, **41**, 91.
14 M. C. Filion and N. C. Phillips, *Biochim. Biophys. Acta*, 1997, **1329**, 345–356.
15 M. C. Filion and N. C. Phillips, *Int. J. Pharm.*, 1998, **162**, 159–170.
16 D. E. Discher and A. Eisenberg, *Science*, 2002, **297**, 967.
17 B. M. Discher, Y.-Y. Won, D. S. Ege, J. C.-M. Lee, F. S. Bates, D. E. Discher and D. A. Hammer, *Science*, 1999, **284**, 1143.
18 G. Battaglia and A. J. Ryan, *J. Am. Chem. Soc.*, 2005, **127**, 8757.
19 G. Battaglia, A. J. Ryan and S. Tomas, *Langmuir*, 2006, **22**, 4910.
20 S. Jain and F. S. Bates, *Macromolecules*, 2004, **37**, 1511.
21 Y.-Y. Won, H. T. Davis and F. S. Bates, *Macromolecules*, 2003, **36**, 953.
22 W. J. Xia and H. Onyuksel, *Pharm. Res.*, 2000, **17**, 612.
23 A. V. Kabanov, E. V. Batrakova, S. Sriadibhatla, Z. Yang, D. L. Kelly and V. Y. Alakov, *J. Controlled Release*, 2005, **101**, 259.
24 P. P. Ghoroghchian, P. R. Frail, K. Susumu, D. Blessington, A. K. Brannan, F. S. Bates, B. Chance, D. A. Hammer and M. J. Therien, *Proc. Natl. Acad. Sci. U. S. A.*, 2005, **102**, 2922–2927.
25 P. J. Photos, L. Bacakova, B. Discher, F. S. Bates and D. E. Discher, *J. Controlled Release*, 2003, **90**, 323–334.
26 F. Ahmed, R. I. Pakunlu, G. Srinivas, A. Brannan, F. Bates, M. L. Klein, T. Minko and D. E. Discher, *Mol. Pharm.*, 2006, **3**, 340.
27 H. Lomas, I. Canton, S. MacNeil, J. Du, S. P. Armes, A. J. Ryan, A. L. Lewis and G. Battaglia, *Adv. Mater.*, 2007, in press.
28 N. A. Alcantar, E. S. Aydil and J. N. Israelachvili, *J. Biomed. Mater. Res.*, 2000, **51**, 343.
29 S. Chen, J. Zheng, L. Li and S. Jiang, *J. Am. Chem. Soc.*, 2005, **127**, 14473.
30 A. Vonarbourg, C. Passirani, P. Saulnier and J.-P. Benoit, *Biomaterials*, 2006, **27**, 4356–4373.
31 J. Du, Y. Tang, A. L. Lewis and S. P. Armes, *J. Am. Chem. Soc.*, 2005, **127**, 17982.
32 A. Napoli, M. Valentini, N. Tirelli, M. Martin and J. A. Hubbell, *Nat. Mater.*, 2004, **3**, 183.
33 F. Ahmed and D. E. Discher, *J. Controlled Release*, 2004, **96**, 37–53.
34 J. J. Lin, P. P. Ghoroghchian, Y. Zhang and D. A. Hammer, *Langmuir*, 2006, **22**, 3975.
35 C. Booth, G.-E. Yu, and V. M. Nace, *Amphiphilic Block Copolymers: Self-Assembly and Applications*, ed. A. Paschalis and L. Bjorn, Elsevier Science Ltd, 2000.
36 A. J. Ryan, J. P. A. Fairclough, I. W. Hamley, S.-M. Mai and C. Booth, *Macromolecules*, 1997, **30**, 1723–1727.
37 D. R. Ralston, C. Layton, A. J. Dalley, S. G. Boyce, E. Freedlander and S. MacNeil, *Br. J. Dermatol.*, 1999, **140**, 605.
38 C. Giacomelli, L. L. Men, R. Borsali, S. P. Armes and A. L. Lewis, *Biomacromolecules*, 2006, **7**, 817.
39 G. Battaglia and A. J. Ryan, *J. Phys. Chem. B*, 2006, **110**, 10272.
40 U. Borchert, U. Lipprandt, M. Bilang, A. Kimpfler, A. Rank, R. Peschka-Süss, R. Schubert, P. Lindner and S. Förster, *Langmuir*, 2006, **22**, 5843.
41 T. Mosmann, *J. Immunol. Methods*, 1983, **65**, 55.
42 G. Battaglia and A. J. Ryan, *Nat. Mater.*, 2005, **4**, 869–876.
43 A. S. Baldwin, *Annu. Rev. Immunol.*, 1996, **14**, 649.
44 G. Battaglia and A. J. Ryan, *Angew. Chem., Int. Ed.*, 2006, **45**, 2052.
45 The aggregation number of a polymersome with radius r and membrane thickness t, can be calculated as the ratio between the polymersome surface area $4\pi(r^2 + (rt)^2)$ and the area per molecule (this can be calculated using the method in ref. 18 and the membrane thickness measured in ref. 31).
46 M. M. Koslov and V. S. Markin, *J. Theor. Biol.*, 1984, **109**, 17.
47 B. L.-S. Mui, P. R. Cullis, E. A. Evans and T. D. Madden, *Biophys. J.*, 1993, **64**, 443.